Electronic Supplementary Material (ESI) for Lab on a Chip.

Supporting Information

Rapid Microfluidics Prototyping Through Variotherm Desktop Injection Molding for Multiplex Diagnostics

Gianmarco D. Suarez,[a] Steevanson Bayer,[a] Yuki Yu Kiu Tang,[c] Domenick A. Suarez,[c] Peter Pak-Hang Cheung[b]* and Stefan Nagl[a]*

[a]Department of Chemistry, The Hong Kong University of Science and Technology, Clear Water Bay, Kowloon, Hong Kong

[b]Department of Chemical Pathology, The Chinese University of Hong Kong, Shatin, New Territories, Hong Kong

[c]Quommni Technologies Limited, Tsuen Wan, New Territories, Hong Kong

*To whom correspondence may be addressed. E-mail: chnagl@ust.hk, ppcheung@cuhk.hk.edu

Table of Contents

Technical Considerations for the Centrifugal Microfluidic Design

The central filling mechanism of the centrifugal microfluidic chip is designed such that excess fluid is released through the gas outlets. This is achieved by designing the gas outlet with a lower capillary pressure than the first valve (i.e., the passive capillary valve between the central chamber and downstream microfluidics). This is done according to the following formula[1,2]:

$$P_S = a\left(\frac{4\gamma}{D_h}\right) + b \qquad (1)$$

where P_S is the capillary pressure, *a* and *b* are empirically determined constants, γ is the liquid's surface tension, and D_h is the channel's hydraulic diameter. Capitalizing on the inverse relationship between hydraulic diameter and capillary pressure, we designed the gas outlet (D_h = 1 mm) to have a capillary pressure approximately less than half that of the first valve (D_h = 0.41 mm). The circular gas outlet thus had a diameter of 1 mm while the dimensions of the first valves were 0.4 mm by 0.42 mm *w* x *h*.

The first and second valve (the second valves separate the metering and reaction chambers) sets were configured to provide a reliable separation of rotational burst frequencies. In guiding our design, we used the following formula[1,2] to determine suitable valve dimensions:

$$P_\omega = \rho\omega^2\bar{r}\Delta r > P_S \qquad (2)$$

where P_ω is the centrifugally induced pressure, ρ is the liquid density, is the rotational frequency, $\bar{r}$ is the mean radial distance of the liquid from the rotational center, Δr is the liquid's radial height. Based on this relation, we determined that for any given angular frequency, P_ω would be 3-fold higher at the second valves as compared to the first valves. Therefore, we selected valve dimensions such that the first valves' hydraulic diameter was 3.4 times as large as that of the second valves, yielding second valves 100 μm wide and 150 μm high.

Design of Custom Imaging Rig

The design of the custom imaging rig drew inspiration from a layout reported by Xue et al.[3] In particular, the aspect of obliquely illuminating the subject while imaging from above was incorporated in order to provide for a straightforward setup of the optics needed to fluorescently image the centrifugal microfluidics. Blue light from a hexagonally arranged array of LEDs was first bandpass filtered into a complementary array of optical light guides (one light guide per LED). The light guides transmitted the excitation light to the reaction chambers of the centrifugal microfluidic chip at an oblique angle, while emissions from the optical pH sensors were filtered and imaged from above (Supp. Fig. 1A). To construct this design, various parts were 3D-printed to properly position the optical components with respect to one another (Supp. Fig. 1B). Ultimately, by using optical light guides, the need for a collimating lens, diffuser, and dichroic mirror was obviated, reducing the cost of the imaging rig and making it compact.

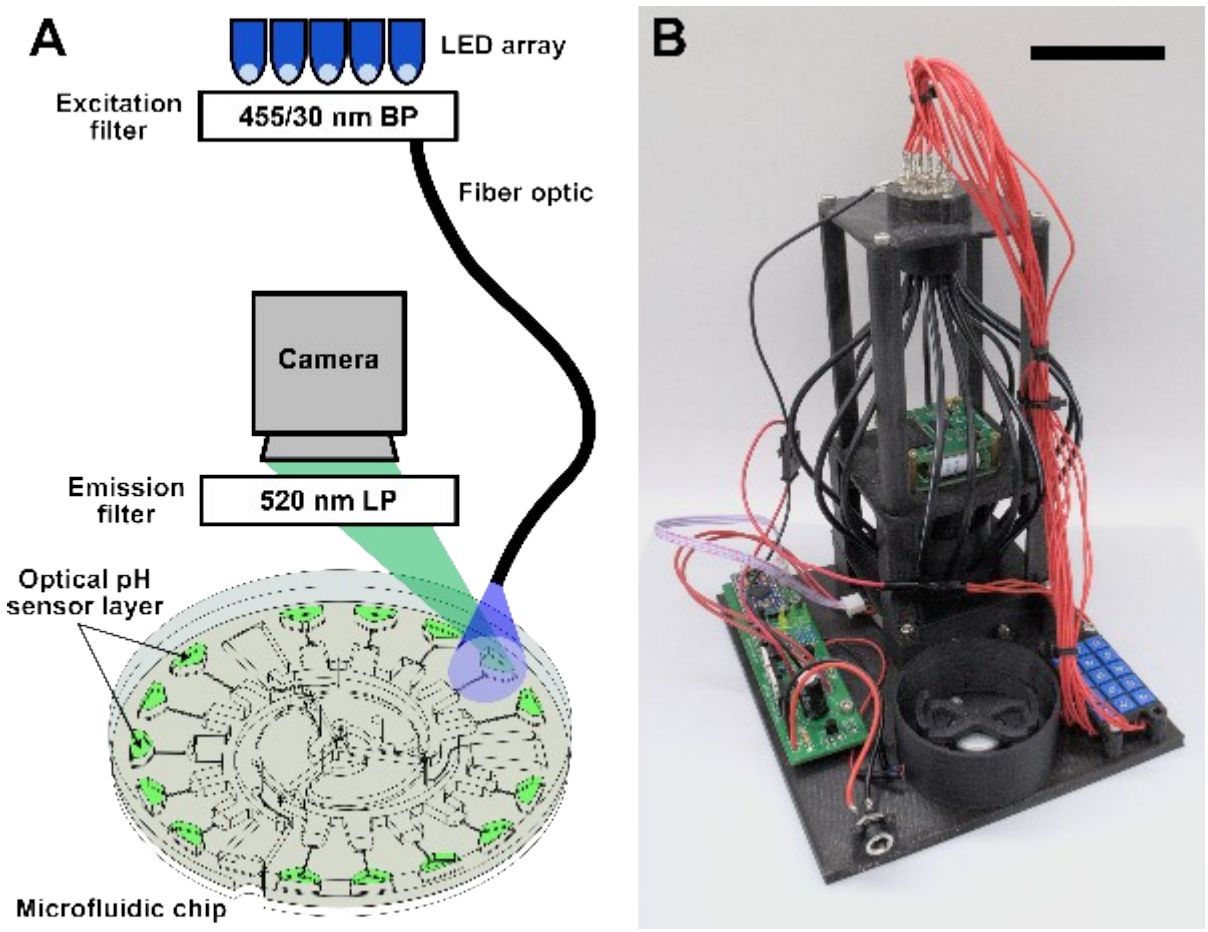

Supplementary Figure 1: a) Diagram of optical components used in imaging rig. b) Photograph of imaging rig. Scale bar is 5 cm.

Aside from positioning the optical components, the 3D-printed parts also supported other essential components of the imaging rig, such as the microcontroller and the heat block. The heat block was designed to slide under the optical assembly (Supp. Fig. 2A), to make loading of the chips easier. To verify the functionality of all these components as assembled, fluorescent control chips were employed. To define regions of interest that correspond to the reaction chambers, a dummy chip was used that had 5 µL of fluorescent green enamel paint (Testors, United States) deposited and dried into the reaction chambers (Supp. Fig. 2B). Using these regions of interest (ROIs), the blue light emission of the individual light guides was adjusted using another fluorescent control made by CNC milling a piece of fluorescent green acrylic (Marga Cipta, Indonesia) into the profile of the microfluidic chips (Supp. Fig. 2C). Since each LED was connected to a separate variable resistor, the blue light each ROI received could be tuned to equalize measured emissions. This was accomplished, with a coefficient of variation of only 0.59 % achieved between the ROIs (Supp. Fig. 2D). This indicated that the optical assembly was suitable for fluorescence measurements during LAMP.

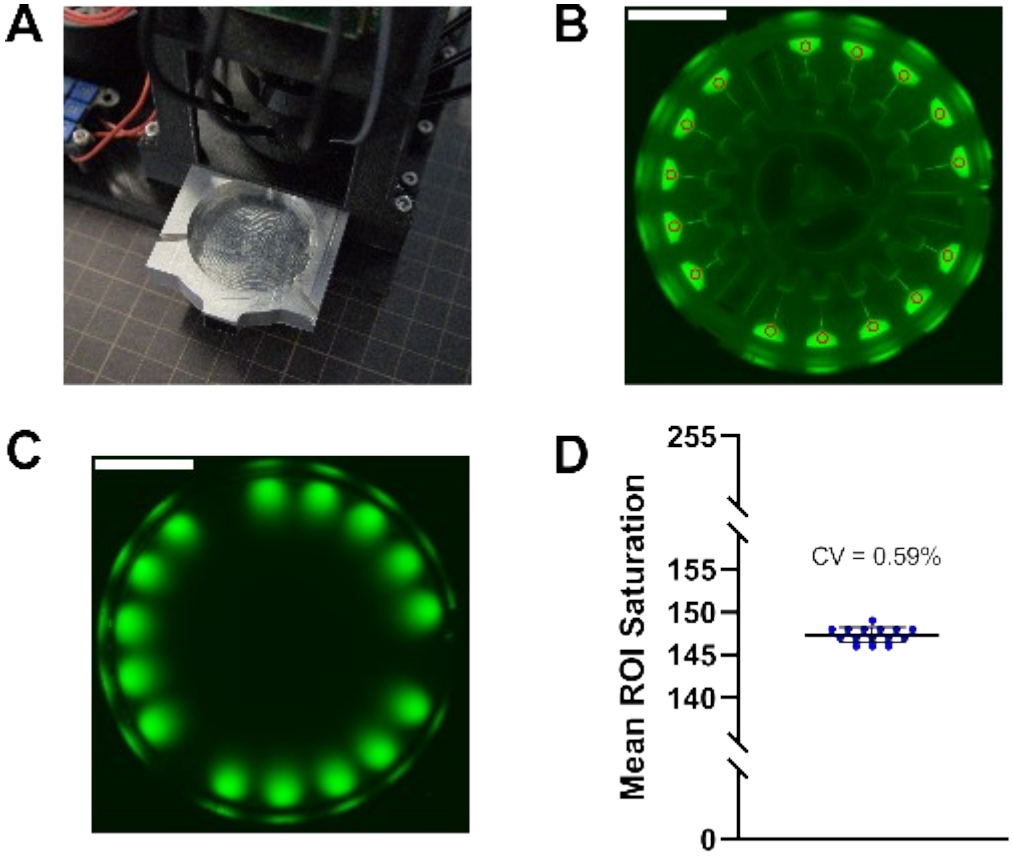

Supplementary Figure 2: a) Heat block extended from imaging rig. Images of b) fluorescent enamel chip control with regions of interest indicated by red circles and c) fluorescent acrylic standard used for calibration. Scale bars are 1 cm. d) Mean saturation of regions of interest on fluorescent acrylic standard.

Fabrication of Injection Molding Assembly

The injection molding assembly was constructed from both custom-milled aluminum parts and standard parts (Supp. Fig. 3A). These standard parts included the pins, guide pins and bushings, and springs. The remaining parts were custom.

The bottom plate served as the base for moveable portion of the assembly and guided the ejector knockout pins. When the platens of the injection molder are moved apart and the mold is opened, these knockout pins engage with an aluminum plate behind the B platen. The ejector knockout pins push the ejector plate, which in turn pushes the ejector return pins, sprue knockout pin, and ejector pins into their corresponding holes within the B plate. The ejector retainer plate is joined with screws and nuts to the ejector plate, to secure the heads of the pins. The springs on the ejector return pins push the ejector retainer plate and ensure the pins are restored to their original position when the mold is closed again. This ejector assembly is contained within a space behind the B plate formed by the spacer blocks.

The ejector return pins are thicker than the ejector pins and serve as guides for the movement of the ejector pins. The ejector pins engage with the molded plastic part and force it from the B cavity of the mold. The sprue knockout pin shears the molded sprue from the annular ring sprue pullers, helping to completely release the part.

The B plate is movable and hosts the B cavity with the microfluidic features, the annular ring sprue puller which removes the sprue and molded part from the A plate, and half of the circular runner which guides molten plastic to the cavities. The A plate is immobile and hosts the A cavity with features that form through-holes in the molded part, the other half of the runner, and the sprue which conducts plastic from the injection barrel to the runner. The A and B plates are aligned to each other with the aid of guide pins and bushings. These pins and bushings are inserted near the corners of the plates and ensure that the cavity halves register correctly. The sprue bushing plate sits between the A plate and the A platen and serves as an adaptor between the injection barrel nozzle and the sprue. The positioning of all these parts and there assembly is illustrated by the perspective diagrams in supplementary figure 3 B,C.

An important consideration in designing the molding assembly is the layout of the platens (Supp. Fig. 4 A,B). The platens had 7 mm wide through-holes which were spaced either 1 or 2 cm from their neighbors, depending on orientation. Therefore, the size and placement of these holes was considered when determining how to place nuts, bolts, and pins for securing the injection molding assembly to the platens and ensuring proper function.

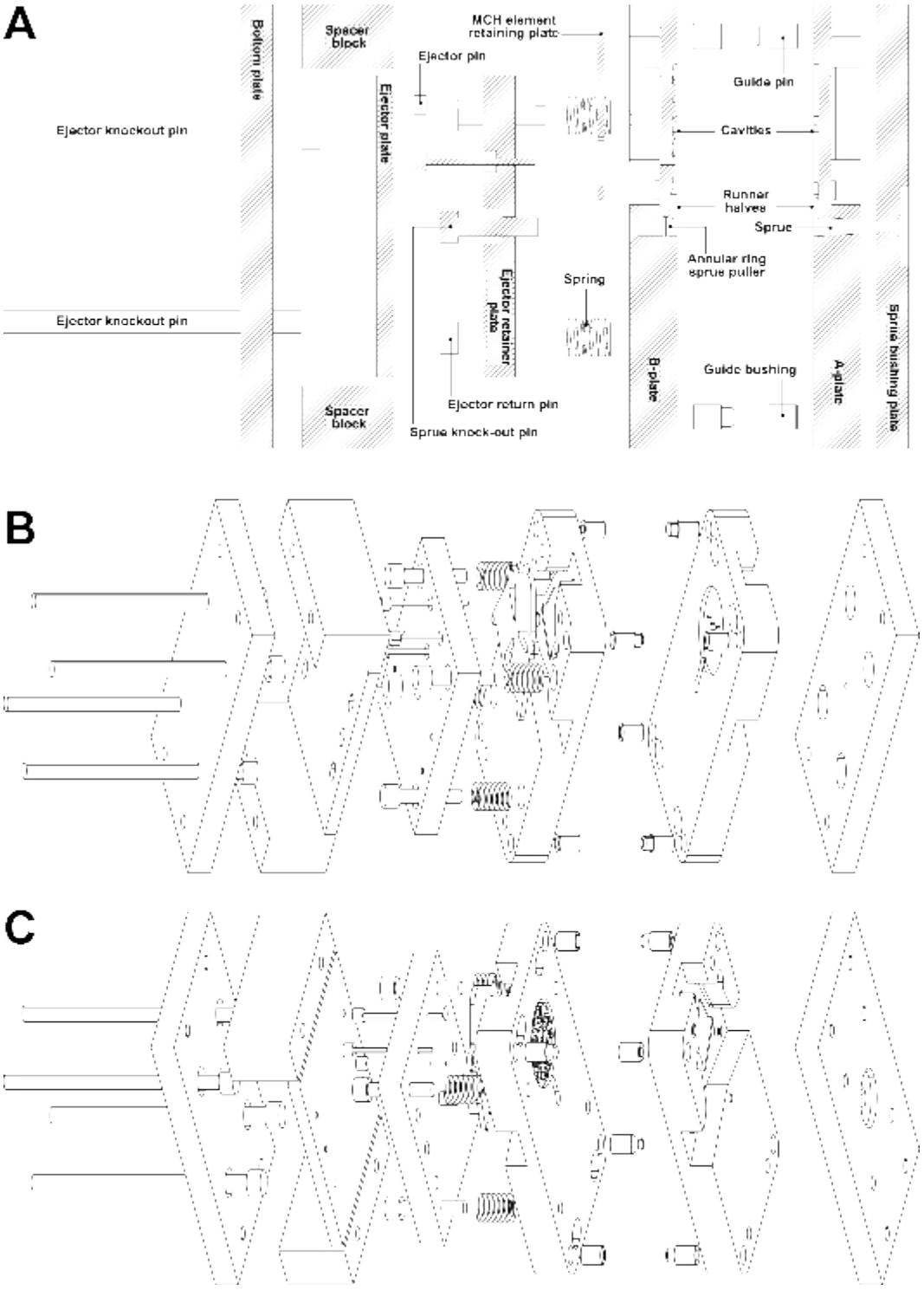

Supplementary Figure 3: a) Cross-sectional diagram of injection molding assembly with parts labeled. Perspective views of exploded injection molding assembly a) facing the A plate and b) facing the B plate.

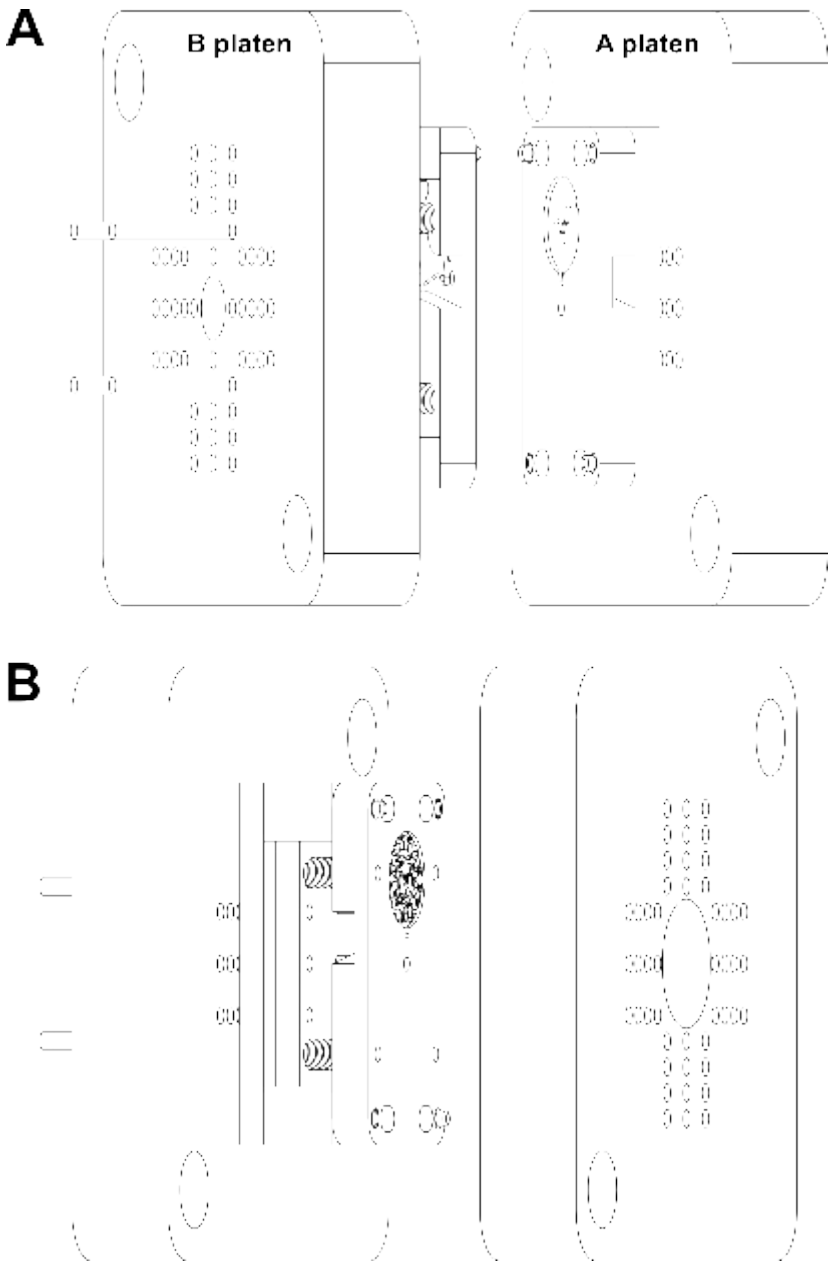

Supplementary Figure 4: Perspective schematics of injection mold assembly mounted on platens showing a) the A plate and b) the B plate.

Supplementary Table 1: A list of FDA-approved medical devices for performing CYCP2C19 genotyping. This list was obtained by searching “CYP2C19” through the Devices@FDA database (https://www.accessdata.fda.gov/scripts/cdrh/devicesatfda/index.cfm).

Device Name	Company	Date Approved	Methodology	Readout
Infiniti CYP2C19 Assay	Autogenomics Incorporated	10/25/2010	PCR and microarray	Fluorescence
Verigene CYCP2C19 Nucleic Acid Test (2C19)	Nanosphere Inc.	11/6/2012	Gold nanoparticle probe and oligo microarray	Fluorescence
Spartan RX CYP2C19 Test System	Spartan Bioscience Inc.	8/12/2013	PCR	Fluorescence
xTAG CYP2C19 Kit v3	Luminex Molecular Diagnostics Inc.	9/11/2013	PCR and bead-based hybridization	Fluorescence
Genomadix Cube CYP2C19 System	Genomadix Inc.	3/21/2023	PCR	Fluorescence

Supplementary Table 2: Machining parameters are listed for the various tools used in this work.

Tool Number	Tool Type	Tool Diameter (mm)	Number of Flutes	Shank Diameter (mm)	Overall Tool Length (mm)	Neck Length (mm)	Horizontal Speed (mm/s)	Vertical Speed (mm/s)	Spindle Speed (rpm)	Stock Material	Flood Coolant?	Operations Used For
1	Square End Mill	6	4	6	50	N/A	10	1	18000	Al (6061-T6)	Yes	Profiling mold plates, machining holes
2	Long-neck Square End Mill	1.5	2	4	50	20	2	0.5	24000	Al (6061-T6)	Yes	Machining ejector pin holes
3	Square End Mill	4	4	4	50	N/A	10	1	24000	Al (6061-T6)	Yes	Machining holes, heating cavities
4	Square End Mill	3	4	3	50	N/A	7.5	0.5	24000	Al (6061-T6)	Yes	Machining holes
5	Square End Mill	2	4	4	50	N/A	5	1	24000	Al (6061-T6)	Yes	Machining holes
6	Square End Mill	1	4	4	50	N/A	1.5	0.5	24000	Al (6061-T6)	Yes	Machining gates
7	Ball End Mill	4	2	4	50	N/A	2.5	0.5	24000	Al (6061-T6)	Yes	Machining runners
8	Square End Mill	0.8	2	4	50	N/A	2	0.5	24000	Al (6061-T6)	Yes	Maching A plate cavity
9	Square End Mill	0.4	2	4	50	N/A	2	0.5	24000	Al (6061-T6)	Yes	Machining B plate cavity
10	Chamfer End Mill	6	3	6	50	N/A	10	1	24000	Al (6061-T6)	Yes	Chamfering B plate pin holes
11	Undercutting End Mill	2	2	4	50	N/A	0.5	0.5	24000	Al (6061-T6)	Yes	Machining annular ring sprue puller
12	Thread Mill	M3	3	4	50	N/A	0.8	0.8	24000	Al (6061-T6)	Yes	Threading holes for mounting MCH element retainer plate
13	O-flute End Mill	1	1	3.175	40	N/A	5	5	2400	Polystyrene	No	Post-processing injection molded parts, cutting plastic substrates
14	O-flute End Mill	2	1	3.175	40	N/A	10	0.5	12000	PMMA	No	Cutting custom fluorescent acrylic standards

Supplementary Table 3: Primer and gene fragment sequences used in this study.

Primer Name	Primer Sequence (5'-3')
WT*2_FIP	CCGGGAAATAATCTTTTAATTTAATAAATTATTGTTTTCTCTTAG
WT*2_BIP	CGGGAACCCGTGTTCTTTTACTTTCTCC
MUT*2_FIP	CTGGGAAATAATCTTTTAATTTAATAAATTATTGTTTTCTCTTAG
MUT*2_BIP	CAGGAACCCGTGTTCTTTTACTTTCTCC
***2_Loop_F**	GATAGTGGGAAAATTATTGC
***2_Loop_B**	CAAATTACTTAAAAACCTTGCTT
***2_F3**	CCAGAGCTTGGCATATTGTATC
***2_B3**	AGGGTTGTTGATGTCCAT
WT*3_FIP	TCCAGGGGTCTTAACTTGATGGAAAAAT
WT*3_BIP	GGATCCAGGCCCAGAAAAAAAGACTGT
MUT*3_FIP	TTCAGGGGTCTTAACTTGATGGAAAAAT
MUT*3_BIP	GAATCCAGGCCCAGAAAAAAGACTGT
***3_Loop_F**	GCTTACAATCCTGATGTT
***3_Loop_B**	GTAAGGCCAAGTTTTTTG
***3_F3**	TCCAGAAACGTTTCG
***3_B3**	AGGGCTTGGTCAATA

Gene Fragment	Sequence (5'-3')
CYP2C19 *2 Fragment	AAATTACAACCAGAGCTTGGCATATTGTATCTATACCTTTATTAAAT GCTTTTAATTTAATAAATTATTGTTTTCTCTTAGATATGCAATAATTT TCCCACTATCATTGATTATTTCCCAGGAACCCATAACAAATTACTT AAAAACCTTGCTTTTATGGAAAGTGATATTTTGGAGAAAGTAAAAG AACACCAAGAATCGATGGACATCAACAACCCTCGGGACTTTATTG ATTGCTTC
CYP2C19 *3 Fragment	CTGCTCCATTATTTTCCAGAAACGTTTCGATTATAAAGATCAGCAA TTTCTTAACTTGATGGAAAAATTGAATGAAAACATCAGGATTGTAA GCACCCCCTGAATCCAGGTAAGGCCAAGTTTTTTGCTTCCTGAGA AACCACTTACAGTCTTTTTTTCTGGGAAATCCAAAATTCTATATTGA CCAAGCCCTGAAGTACATTTTTGAATACTACAGTCTTGCCTAGACA GCCATGGGGT
CYP2C19 WT Dual Fragment	GTGATCTGCTCCATTATTTTCCAGAAACGTTTCGATTATAAAGATC AGCAATTTCTTAACTTGATGGAAAAATTGAATGAAAACATCAGGAT TGTAAGCACCCCCTGGATCCAGGTAAGGCCAAGTTTTTTGCTTCC TGAGAAACCACTTACAGTCTTTTTTTCTGGGAAATCCAAAATTCTA TATTGACCAAGCCCTGAAGTACATTTTTGAATACTACAGTCTTGCC TAGACAGCCATGGGGTAAATTACAACCAGAGCTTGGCATATTGTA TCTATACCTTTATTAAATGCTTTTAATTTAATAAATTATTGTTTTCTC TTAGATATGCAATAATTTTCCCACTATCATTGATTATTTCCCGGGAA CCCATAACAAATTACTTAAAAACCTTGCTTTTATGGAAAGTGATATT TTGGAGAAAGTAAAAGAACACCAAGAATCGATGGACATCAACAAC CCTCGGGACTTTATTGATTGCTTCCTGAT

Supplementary Table 4: Average time to results (TTR) for AS-LAMP genotyping reactions.

Allele Analog	TTR (minutes)
*2 WT	35.3
*2 Mutant	40.6
*3 WT	45.3
*3 Mutant	32.0

Supplementary References

1 R. Gorkin, J. Park, J. Siegrist, M. Amasia, B. S. Lee, J. M. Park, J. Kim, H. Kim, M. Madou and Y. K. Cho, *Lab Chip*, 2010, **10**, 1758–1773.

2 D. C. Duffy, H. L. Gillis, J. Lin, N. F. Sheppard and G. J. Kellogg, *Anal. Chem.*, 1999, **71**, 4669–4678.

3 Y. Xue, I. G. Davison, D. A. Boas and L. Tian, *Sci. Adv.*, 2020, **6**, eabb7508.